

Short communication

^{57}Fe Mössbauer spectroscopy and surface modification with zinc and magnesium of $\text{LiCo}_{0.8}\text{Fe}_{0.2}\text{MnO}_4$ 5 V electrodes

R. Alcántara^{a,*}, M. Jaraba^a, P. Lavela^a, J.L. Tirado^a, J.C. Jumas^b, J. Olivier Fourcade^b

^a *Laboratorio de Química Inorgánica, Universidad de Córdoba, Edificio C3, Planta 1, Campus de Rabanales, 14071 Córdoba, Spain*

^b *Laboratoire des Agrégats Moléculaires et Matériaux Inorganiques, UMR 5072, Université Montpellier II, CC 15, Place Eugène Bataillon, 34095 Montpellier Cedex 5, France*

Received 28 January 2004; accepted 22 March 2004

Available online 23 July 2004

Abstract

A high-voltage (5 V) $\text{LiCo}_{0.8}\text{Fe}_{0.2}\text{MnO}_4$ electrode with spinel-type structure has been prepared. ^{57}Fe Mössbauer spectra reveal high-spin Fe^{3+} ions in octahedral coordination in the pristine sample, which are oxidized to tetravalent iron ions. Surface treatments with zinc and magnesium have been applied. Zinc and magnesium were homogeneously distributed, according to EPMA and mapping analysis, while the spinel structure is maintained. The magnesium and the zinc treatments drive to better electrochemical performance and capacity retention. © 2004 Elsevier B.V. All rights reserved.

Keywords: ^{57}Fe Mössbauer spectroscopy; Lithium batteries; X-ray diffraction

1. Introduction

A renewed concept of lithium-ion battery has been proposed in the last few years, which is based on a high-voltage cathode working at ca. 4.6–5.2 V versus Li^+/Li , and an anode that works about 1 V [1–5]. The safety problems related with lithium compounds of graphitic materials formed near 0 V versus Li^+/Li would be avoided in this new generation of lithium-ion batteries.

At this moment, the phosphate-based [6] and the manganese-containing spinels [4] can be cited as the most successful 5 V electrodes. In the case of the manganese spinels, which can be considered as derived from LiMn_2O_4 , the 5 V operation voltage is achieved with partial manganese substitution by nickel [4], cobalt [7], iron [8] or combination of these elements [9,10].

One of the drawbacks to overcome is the electrolyte decomposition that takes place by irreversible reaction with the positive electrode in the charged state [11], this effect being more marked when temperature is high (i.e. more than 50 °C), and it drives to capacity fade on cycling. Hence, the development of suitable electrolytes is a key factor for the effective use of these batteries. Another way to focus this problem is the optimization of the cathode materials, by en-

hancing their stability in the actually used electrolytes. In the case of the LiPF_6 -based electrolytes the presence of HF, which is formed by reaction of the salt with traces of water, favors the chemical attack and corrosion of the electrode. One possibility is to use low-surface electrodes to minimize the possibility of irreversible reactions at the surface. A second way is the chemical modification of the surface. In this sense, several studies have shown the positive effect of the coating and surface treatments on cathodes which operate at 4 or 5 V [12–20].

On the other hand, ^{57}Fe Mössbauer spectroscopy has been applied to study different electrode materials with spinel-type structure [8,21].

The two aims of this work are to study the mechanism of the oxidation of $\text{LiCo}_{0.8}\text{Fe}_{0.2}\text{MnO}_4$ by ^{57}Fe Mössbauer spectra, and the surface modification of this 5 V cathode by coating with zinc and magnesium.

2. Experimental

The $\text{LiCo}_{0.8}\text{Fe}_{0.2}\text{MnO}_4$ sample was obtained as described in elsewhere [9] by heating a solid precursor at 800 °C during 72 h, and re-heating at 600 °C during 48 h. The chemical composition of the obtained product was checked by atomic absorption spectroscopy and electron-probe microanalysis (EPMA). To obtain adequate ^{57}Fe Mössbauer

* Corresponding author. Tel.: +34-957-218637; fax: +34-957-218621. E-mail address: iq2alror@uco.es (R. Alcántara).

spectra, a 97% ^{57}Fe -enriched sample was prepared. For this purpose metallic ^{57}Fe iron was dissolved, precipitated as iron oxalate, and thus the obtained iron oxalate was used to prepare $\text{LiCo}_{0.8}\text{Fe}_{0.2}\text{MnO}_4$.

For the preparation of the surface modified cathode materials the experimental procedure was as follows. Firstly, the pristine $\text{LiCo}_{0.8}\text{Fe}_{0.2}\text{MnO}_4$ active cathode material was added to a vessel with water, and then continue stirring was applied. Secondly, selected reagents (zinc acetate or magnesium acetate) were added, followed by strong stirring at room temperature for several hours until dryness. The quantities of the reagents were calculated to obtain that the weight of ZnO, or MgO, be 1.5% of the bare cathode. Finally, the mixture constituted by the cathode and the additive was annealed at 400 °C during 1 h in air.

X-ray diffraction (XRD) patterns were recorded on a Siemens D5000 instrument equipped with graphite monochromator and using Cu K α radiation. SEM micrographs and EPMA were obtained in a JEOL-JSM6300 instrument. The FT-IR spectra were recorded in an FT-MIR-Magna-IR550-Series II instrument using KBr pellets.

^{57}Fe Mössbauer spectra were obtained at room temperature with an EG&G constant accelerator spectrometer in transmission mode. The source of nominal activity of 10 mCi was ^{57}Fe in an Rh matrix. The velocity scale was calibrated from the magnetic sextuplet of a high-purity iron foil absorber. Ex situ measurements were performed on the electrodes at several depths of charge and discharge. For this purpose the Swagelok cells were opened inside the glove box and the electrodes containing the active material were placed in a special sample holder which was transparent to the γ -rays. The effective thickness of the absorber was about 2 mg of ^{57}Fe cm $^{-2}$. Experimental data were fitted to Lorentzian lines by using a least-squares-based method [22]. The goodness of the fit was controlled by the classical test of χ^2 . All the isomer shifts are given relative to the center of the α -Fe spectrum at room temperature.

^7Li MAS NMR spectra were recorded in a Bruker Avance400WB instrument with rotor of 4 mm diameter.

The electrochemical behavior of the materials was tested at room temperature by using two-electrode SwagelokTM cells of the type $\text{Li}|\text{LiPF}_6(\text{EC}:\text{DEC})|\text{LiCo}_{0.8}\text{Fe}_{0.2}\text{MnO}_4$. The positive electrodes, having about 6 mg cm $^{-2}$ of active material supported onto an aluminum foil, were prepared as 9 mm diameter disks by drying at 120 °C into vacuum at least for 2 h and pressing then a mixture of 86% of the active oxide, 6% of PVDF binder, and 8% of carbon (50% weight mixture of graphite and carbon black). Lithium electrodes consisted of a clean 9 mm diameter lithium metal disk. The commercial (Merck LP40) electrolyte solution 1 M LiPF_6 in a 1:1 (w/w) mixture of ethylene carbonate (EC) and diethyl carbonate (DEC) was supported by porous glass-paper discs WhatmanTM. The electrochemical charge/discharge curves were obtained by galvanostatic cycling, using a multichannel MacPile II system, at

C/5 rate, i.e. one Li extracted from $\text{LiCo}_{0.8}\text{Fe}_{0.2}\text{MnO}_4$ in 5 h.

3. Results and discussion

3.1. ^{57}Fe Mössbauer

^{57}Fe -enriched $\text{LiCo}_{0.8}\text{Fe}_{0.2}\text{MnO}_4$ sample exhibits a Mössbauer spectrum constituted by one doublet (Fig. 1). The fitting of this spectrum gives the following Mössbauer parameters: isomer shift $\text{IS1} = +0.332$ mm s $^{-1}$ and quadrupolar splitting $\text{QS1} = 0.75$ mm s $^{-1}$ (Table 1). Signals corresponding to impurities are not observable. This spectrum is ascribed to Fe^{3+} with high-spin configuration in octahedral coordination, which is in agreement with previous diffraction results [9]. By electrochemical oxidation of the electrode (C/20 rate) up to 4.9, 5.0 and 5.1 V, the spectra change and two new signals appear between +0.05 and +0.01 mm s $^{-1}$ (IS2) and between -0.01 and +0.11 mm s $^{-1}$ (IS3). Since both IS2 and IS3 signals are in the range of tetravalent iron, this evidences that the oxidation of Fe^{3+} to Fe^{4+} during charge is occurring, in agreement with previous results of iron-containing manganese spinels [8] and

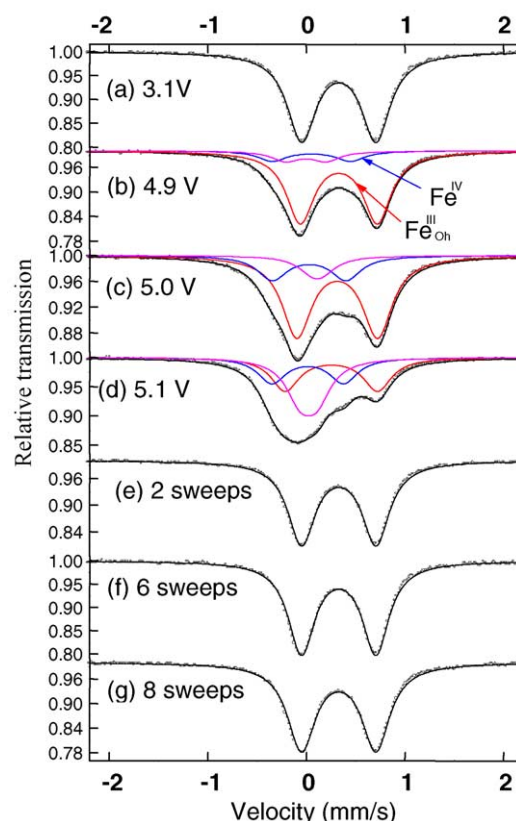


Fig. 1. ^{57}Fe Mössbauer spectra of (a) pristine $\text{LiCo}_{0.8}\text{Fe}_{0.2}\text{MnO}_4$, (b) after first charge to 4.9 V, (c) first charge to 5.0 V, (d) first charge to 5.1 V, (e) at 3.1 V after two cycles, (f) at 3.1 V after six cycles and (g) at 3.1 V after eight cycles.

Table 1
 ^{57}Fe Mössbauer parameters evolution of $\text{Li}_x\text{Co}_{0.8}\text{Fe}_{0.2}\text{MnO}_4$ electrodes

Cycle	Q	IS1	QS1	Γ 1	C1	IS2	QS2	Γ 1	C2	IS3	QS3	Γ 1	C3	χ^2
0	0	0.33	0.75	0.35	100									1.29
0	115	0.33	0.78	0.34	78	0.05	0.79	0.34	11	-0.01	0.41	0.34	11	1.03
0	145	0.31	0.82	0.36	68	0.03	0.75	0.36	21	0.11	0.09	0.36	11	1.09
0	190	0.25	0.94	0.34	35	0.01	0.73	0.34	27	0.02	0.17	0.34	38	0.78
1	0	0.33	0.75	0.34	100									1.46
3	0	0.33	0.75	0.33	100									1.25
4	0	0.33	0.75	0.34	100									1.10

Q : charge capacity (mAh g^{-1}); IS: isomer shift (mm s^{-1}) relative to $\alpha\text{-Fe}$; QS: quadrupole splitting (mm s^{-1}); Γ : full width at half maximum (mm s^{-1}) with natural width equal to 0.19 mm s^{-1} ; C: contribution in percentage; χ^2 : fitting parameter.

with iron-substitute lithium nickelate [23]. The relative contribution of trivalent iron (C1) decreases from 4.9 to 5.1 V, while the contributions of the tetravalent irons (C2 and C3) increase. The assignation of the two tetravalent irons is a difficult task, and it could be due to a distribution of sites as a consequence of the neighbor tetrahedral Li or vacancies or, alternatively, to the coexistence of high-spin and low-spin Fe^{4+} . In addition, since quadrupole splitting is not constant at the different states of charge, then a variation in the iron environment happens. In fact, the contraction of the unit cell during lithium extraction has been reported for several transition metals spinel-type oxides that work in the 5 V region [9,10]. Structural stability is evidenced by no changes in the spectra from the pristine sample (cycle number 0 in Table 1) until one, three and four complete charge/discharge cycles, where the same IS and QS are found. Irrespectively of this apparent stability regarding the Mössbauer results, capacity loss is observed upon cycling due to irreversible reactions with the electrolyte at the electrode surface as is discussed in Section 3.2.

3.2. Surface treatment

We have previously reported elsewhere XRD and neutron diffraction data of $\text{LiCo}_x\text{Fe}_y\text{Mn}_{2-(x+y)}\text{O}_4$ compounds [9]. Thus, pristine $\text{LiCo}_{0.8}\text{Fe}_{0.2}\text{MnO}_4$ is known to be a cubic spinel with a unit cell parameter of 8.0896_6 \AA . The XRD pattern in Fig. 2 reveals traces of Co_3O_4 spinel as impurity. After surface treatment with zinc and magnesium, no new XRD reflections are observed (Fig. 2). The cubic lattice parameter of $\text{LiCo}_{0.8}\text{Fe}_{0.2}\text{MnO}_4$ (8.0896_6 \AA) slightly decreases after the treatments with magnesium (8.080_3 \AA) and zinc (8.076_2 \AA). This suggests only some minor incorporation of magnesium and zinc in the spinel lattice.

In contrast with $\text{LiNi}_{0.5}\text{Mn}_{1.5}\text{O}_4$, related spinel solid solutions containing cobalt exhibit in the scanning microscope sub-micron particles with irregular shapes [9,10]. Similar irregular shapes and ca. $0.5 \mu\text{m}$ average size of the primary particles were obtained for $\text{LiCo}_x\text{Fe}_y\text{Mn}_{2-(x+y)}\text{O}_4$ compounds (not shown). The small and non-uniform size of the $\text{LiCo}_{0.8}\text{Fe}_{0.2}\text{MnO}_4$ particles can origin enhanced irreversible reactions with the electrolyte. For surface-treated samples, the EPMA mapping showed that zinc and magne-

sium were distributed uniformly all over the powdered samples.

The FT-IR spectrum of bare $\text{LiCo}_{0.8}\text{Fe}_{0.2}\text{MnO}_4$ exhibits two broad bands between 400 and 700 cm^{-1} , which are characteristic of disordered spinels and, typically, those containing iron (Fig. 3). These bands remained unaltered after treatment with zinc and magnesium acetates.

^7Li MAS NMR spectra of bare and zinc-coated samples are shown in Fig. 4. The spectra contain a large number of high-intensity spinning side bands (SSB). The main cause of the large SSB is the dipolar coupling between the lithium nuclei and the unpaired electrons of the paramagnetic ions [24]. From different MAS spectra recorded at 12.0, 14.5 and 30.0 kHz , the main signal in the spectra was identified at about 540 ppm . This value is in agreement with previous results obtained by ^6Li [9]. The location of the main signal is typical of Li^+ in the oxygen tetrahedron environment of the spinel structure [9,24]. After treatment with zinc, no new signals are observed (Fig. 4) and lithium environment is basically unchanged.

In summary, the diffraction and spectroscopic results evidence that the spinel framework is maintained unaltered after surface treatment. Most of the magnesium and zinc content

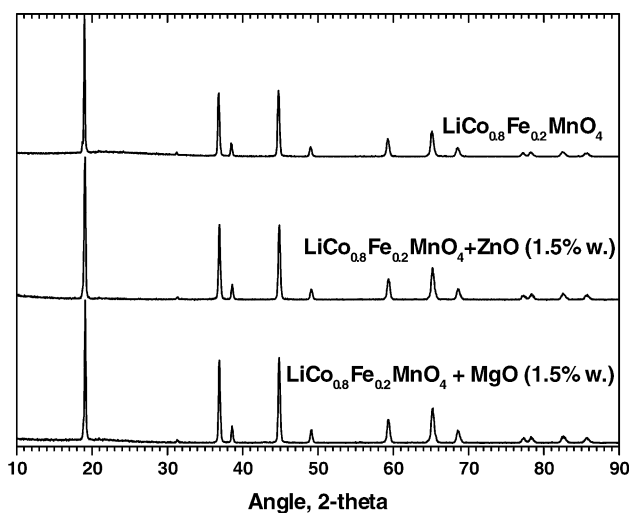


Fig. 2. XRD of bare $\text{LiCo}_{0.8}\text{Fe}_{0.2}\text{MnO}_4$ and after the surface treatment with zinc and magnesium.

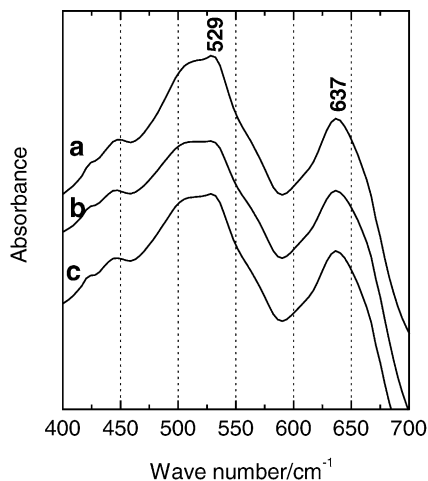


Fig. 3. FT-IR of (a) bare $\text{LiCo}_{0.8}\text{Fe}_{0.2}\text{MnO}_4$ sample and after treatment with (b) zinc and (c) magnesium.

is then expected at the surface in the form of XRD undetectable oxides, which could serve as a protective coating layer. In addition, some minor incorporation of magnesium and zinc in the spinel lattice is suggested by the changes in unit cell parameters. However, the effects of this incorporation on the lattice vibrations or the ^7Li chemical shifts are negligible.

3.3. Electrochemistry

Galvanostatic charge/discharge curves of bare and coated $\text{LiCo}_{0.8}\text{Fe}_{0.2}\text{MnO}_4$ samples in lithium cells are shown in Fig. 5. Most of the exhibited capacity is developed in the 5 V region, except for a short 4 V region with less than 9 mA h g^{-1} . The 5 V region can be ascribed to both $\text{Fe}^{3+}/\text{Fe}^{4+}$ and $\text{Co}^{3+}/\text{Co}^{4+}$ redox couples, while the 4 V region corresponds to $\text{Mn}^{3+}/\text{Mn}^{4+}$. A continuous varia-

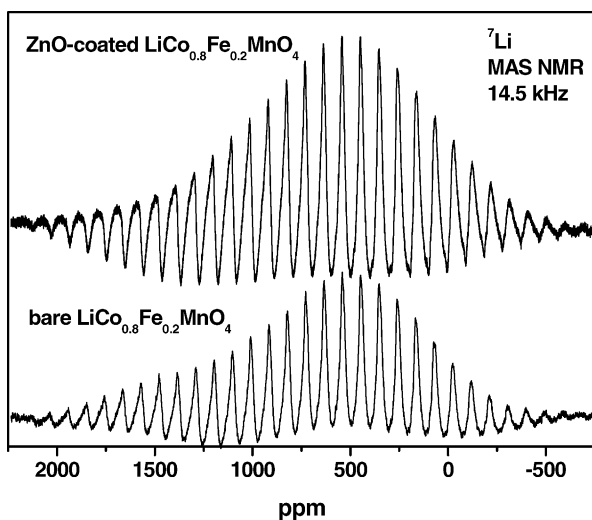


Fig. 4. ^7Li MAS NMR spectra of bare $\text{LiCo}_{0.8}\text{Fe}_{0.2}\text{MnO}_4$ sample and after treatment with zinc; spinning speed is 14.5 kHz.

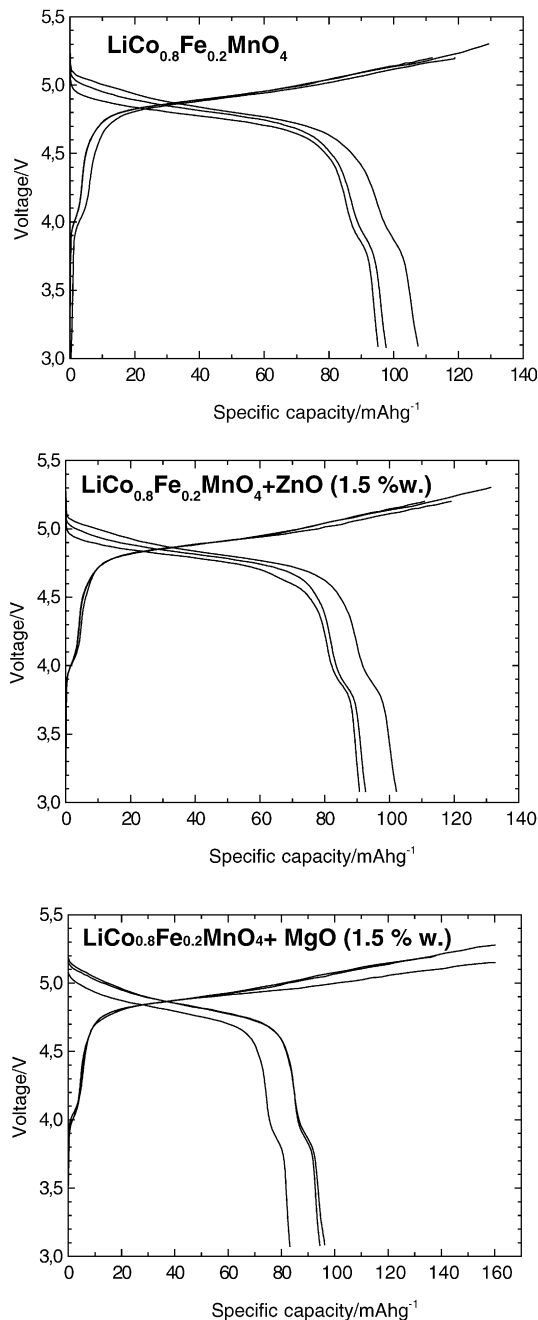


Fig. 5. Galvanostatic charge/discharge cycles (numbers 1–3) of $\text{Li}/\text{LiPF}_6(\text{EC}:\text{DEC})/\text{LiCo}_{0.8}\text{Fe}_{0.2}\text{MnO}_4$ cells and corresponding materials after surface modification with zinc and magnesium; rate: C/5.

tion of the voltage is observed instead of a plateau in the region near 5 V, which agrees with the fact that lithium extraction takes place accompanied by a contraction of the unit cell parameter in a single cubic phase mechanism [9]. In contrast, two cubic phases are observed in an almost constant voltage region at ca. 4.7 V during the extraction of the lithium from $\text{LiNi}_{0.5}\text{Mn}_{1.5}\text{O}_4$ [25]. The nearly constant slope above 5 V of the charge branches of the voltage versus capacity curves for cobalt containing spinels can be related to more extended electrolyte decomposition due

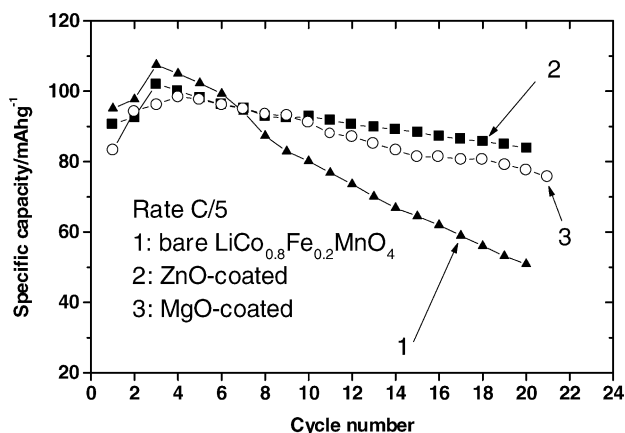


Fig. 6. Capacity evolution upon cycling of Li/LiPF₆(EC:DEC)/LiCo_{0.8}Fe_{0.2}MnO₄ cells and cathode material treated with zinc and magnesium.

to the higher voltage in which Co³⁺ is oxidized. Fig. 6 shows that the initial reversible capacity at C/5 rate is 109 mA h g⁻¹, but it decreases strongly in the first few cycles for bare LiCo_{0.8}Fe_{0.2}MnO₄. This behavior is usual for cobalt-containing 5 V electrodes [10], and the degradation of capacity takes place irrespectively of the local structural stability shown by the ⁵⁷Fe Mössbauer spectra, as discussed above. Apparently, the voltage versus capacity curve (Fig. 5) remains unchanged after coating. However, the surface treatments with zinc and magnesium improve the electrochemical performance significantly (Fig. 6). This evidences that the surface treatments have a protective effect towards the irreversible reactions with the electrolyte, this effect being more evident by using zinc as compared to magnesium. These results show that the protective coatings can be effectively applied to 5 V materials different from other previously reported [16–19,26].

4. Conclusions

High-spin Fe³⁺ ions in octahedral coordination are found in the LiCo_{0.8}Fe_{0.2}MnO₄ spinel-type sample, which are oxidized to Fe⁴⁺ ions in lithium cells in the 5 V region. The application of the coating treatments with zinc and magnesium to this 5 V electrode improves its capacity retention. A protective layer of zinc and magnesium oxides is formed at the electrode surface. This effect seems to be of general applicability for 5 V electrodes.

Acknowledgements

The authors acknowledge financial support from EC (Contract ENK6-CT2000-00082) and MCYT (Contracts MAT2000-2721-CE and MAT2002-00434). R.A. is indebted to MCYT (Programa Ramón y Cajal).

References

- [1] F. Bonino, S. Panero, D. Satolli, B. Scrosati, J. Power Sources 97–98 (2001) 389.
- [2] Y. Xia, T. Sakai, T. Fujieda, M. Wada, H. Yoshinaga, Electrochem. Solid State 4 (2001) A9.
- [3] T. Ohzuku, K. Ariyoshi, S. Yamamoto, Y. Makimura, Chem. Lett. (2001) 1270.
- [4] Q. Zhong, A. Bonakdarpour, M. Zhang, Y. Gao, J.R. Dahn, J. Electrochem. Soc. 144 (1997) 205.
- [5] S. Panero, D. Satolli, M. Salomon, B. Scrosati, Electrochem. Commun. 2 (2002) 810.
- [6] K. Amine, H. Yasuda, M. Yamachi, Electrochem. Solid State 3 (2000) 178.
- [7] H. Kawai, M. Nagata, H. Kageyama, H. Tukamoto, A.R. West, Electrochim. Acta 45 (1999) 315.
- [8] T. Ohzuku, K. Ariyoshi, S. Takeda, Y. Sakai, Electrochem. Acta 46 (2001) 2327.
- [9] R. Alcántara, M. Jaraba, P. Lavela, J.L. Tirado, Chem. Mater. 15 (2003) 1210.
- [10] R. Alcántara, M. Jaraba, P. Lavela, J.L. Tirado, J. Electrochem. Soc. 151 (2004) A53.
- [11] D. Guyomard, J.M. Tarascon, J. Power Sources 54 (1995) 92.
- [12] M. Mladenov, R. Stoyanova, E. Zhecheva, S. Vassilev, Electrochem. Commun. 3 (2001) 410.
- [13] L. Liu, Z. Wang, H. Li, L. Chen, X. Huang, Solid State Ionics 152 (2002) 341.
- [14] H.J. Kweon, S.J. Kim, D.G. Park, J. Power Sources 88 (2000) 255.
- [15] Z. Zheng, Z. Tang, Z. Zahng, W. Sheng, Y. Lin, Solid State Ionics 148 (2002) 317.
- [16] Y.K. Sun, Y.S. Lee, M. Yoshio, K. Amine, Electrochem. Solid State 5 (2002) A99.
- [17] Y.K. Sun, K.J. Hong, J. Prakash, K. Amine, Electrochem. Commun. 4 (2002) 344.
- [18] Y.K. Sun, C.S. Yoon, I.H. Oh, Electrochim. Acta 48 (2003) 503.
- [19] J. Cho, Y.J. Kim, T.J. Kim, B. Park, Angew. Chem. Int. Ed. Engl. 40 (2001) 3367.
- [20] Z. Chen, J.R. Dahn, Electrochem. Solid State 5 (2002) A213.
- [21] R. Alcántara, M. Jaraba, P. Lavela, J.L. Tirado, J.C. Jumas, J. Olivier Fourcade, Electrochem. Commun. 5 (2003) 16.
- [22] W. Künding, Nucl. Instrum. Methods 75 (1969) 336.
- [23] C. Delmas, G. Prado, A. Rougier, E. Suard, L. Fournés, Solid State Ionics 135 (2000) 71.
- [24] C.P. Grey, Y.J. Lee, Solid State Sci. 5 (2003) 883.
- [25] R. Alcántara, M. Jaraba, P. Lavela, J.L. Tirado, Electrochim. Acta 47 (2002) 1829.
- [26] R. Alcántara, M. Jaraba, P. Lavela, J.L. Tirado, J. Electroanal. Chem. 566 (2004) 187.